Mixing, Reaction, and Precipitation: Interaction by Exchange with Mean Micromixing Models

Narayan S. Tavare
Dept. of Chemical Engineering, University of Manchester Institute of Science and Technology, Manchester M60 1QD, United Kingdom

An analysis of interaction by exchange with the mean micromixing model is extended to a process involving elementary chemical reaction between two species and subsequent crystallization of product in a continuous mixed suspension mixed product removal crystallizer. Two specific feed conditions are considered: premixed and unpremixed feeds are considered. The sensitivity of these two cases to several parameters like the Damköhler number, micromixing parameter, fractional flow rate, and dimensionless inlet concentration of excess reactant is explored. Both reaction and crystallization performance characteristics are significantly influenced by the feed conditions. Results for the case of premixed feeds tend to suggest that the model description may be better suited to a nearly segregated configuration.

Introduction

Micromixing (mixing on the molecular scale) can significantly influence the overall performance of a continuous crystallizer. Danckwerts (1958) has specifically pointed out the significance of micromixing in a precipitation system. Process simulation studies concerning the extreme levels of micromixing (Becker and Larson, 1969; Garside and Tavare, 1984, 1985; Tavare, 1986, 1989) have clearly demonstrated this enormous effect and stressed the importance of characterizing micromixing effects from both theoretical and practical viewpoints in a real vessel at some intermediate level. The kinetic events for crystallization systems are generally nonlinear; crystallizers are usually operated at relatively high yields; the residence time distribution (RTD) function is closer to an exponentially decaying type representing a fully backmixed vessel; the physical nature of the crystallization process allows the practical possibility of segregation and therefore micromixing effects may tend to be important in real crystallizers.

Although a variety of micromixing models for a chemical reactor have been proposed by many authors in the chemical reaction engineering literature, published work on such a system is beginning to emerge only recently using the approaches developed in chemical reaction engineering. Pohorecki and Baldyga (1979, 1983a) attempted to develop a model in order to characterize a micromixing level based on the spectral interpretation of mixing in an isotropic homogeneous turbulent field and evaluate the influence of mixing intensity on product precipitate and its crystal-size distribution (CSD) in an agitated vessel for a fast reactive system. They used a micromixing model based on continuous mass transfer between a point and its environment to describe the molecular dissipation zone as originally proposed by Costa and Trevissoi (1972a,b) and demonstrated the influence of mixing on a precipitation process. Tavare (1986), in his intensive review on mixing in continuous crystallizers, cataloged the major types of models that have appeared in the chemical reaction engineering literature in order to judge their applicability to crystallizer configurations. As there is no general acceptance as to what constitutes a sufficient description of micromixing, a host of models describing specific mixing histories has been proposed for chemical reactors, each being an attempt to represent conceivable extreme or intermediate micromixing states with or without some mechanistic implications. Some of these micromixing models can be used for reactive precipitation processes.

Formulation of models for complete segregation and maximum mixedness for a continuous precipitator with any residence time distribution function, as depicted by plug-flow

Present address of N. S. Tavare: Dept. of Chemical Engineering, University of Bradford, West Yorkshire BD7 1DP, England.

vessels with side exits and side entrances, respectively, represents the intrinsic micromixing level in an environment (Danckwerts, 1958; Zwietering, 1959). Environmental models for chemical reactors are essentially system-specific and empirical in nature. Several variations of these environment models for chemical reactors have been proposed, differing either in structure of environment interaction or in transfer rates. For the case of barium sulfate precipitation with premixed feed, Baldyga and Pohorecki (1986) employed a two-environment model under the simplified assumption that nucleation was a dominant process in the completely segregated entering environment, whereas only crystal growth occurred in the maximally mixed leaving environment. Effects of residence time, inlet concentration of reactants, and micromixing parameter on the product precipitate were evaluated and compared with the experimental results obtained for the precipitation of barium sulfate crystals in order to assess the adequacy of the models. Tavare (1992) extended the two-environment model for a reactive precipitation process involving an elementary chemical reaction between two reactant species and subsequent crystallization of a product in a continuous crystallizer with premixed feeds. He also explored the sensitivity of the model to several process parameters.

Pohorecki and Baldyga (1988) investigated the influence of micromixing on the course of the precipitation process associated with an instantaneous irreversible chemical reaction between two ionic solutions. They employed a micromixing model based on the theory of turbulent mixing in a homogeneous isotropic turbulent field to demonstrate that the micromixing intensity and feed conditions were the major factors affecting product characteristics. Villermaux (1990) presented an approach of mathematical modeling of the design of industrial precipitators and to account for the mixing influence on product quality. Most recent studies appear to deal with batch or semibatch reactive precipitation processes (Kuboi et al., 1986; Tosun, 1988; Baldyga et al., 1990; Tovistiga and Wirges, 1990; Marcant and David, 1991, 1993, 1994; Aslund and Rasmuson, 1992; Baldyga, 1993; Podgorska et al., 1993; Iyer and Przybycien, 1994) rather than with continuous operation (Fitchett and Tarbell, 1990; Mydlarz et al., 1992; Tavare, 1993).

The whole gamut of these articles provides detailed analyses of some of the important micromixing models from a theoretical or predictive viewpoint and consequently assesses their suitability to real crystallization systems. The object of this article is to initiate the series by extending the study of interaction by exchange with the mean (IEM) model to a reactive precipitation system. This type of model has been proposed by several authors (Harada et al., 1962; Villermaux and Devillion, 1972; Costa and Trevissoi, 1972a,b; David and Villermaux, 1975, 1983; Plasari et al., 1978; Klein et al., 1980; Villermaux, 1981, 1986; Pohorecki and Baldyga, 1983b,c; Call and Kadlec, 1989) to represent partially segregated chemical reactors. These models are chosen because of their simplicity, versatility and computational economy. The scope of the present study is restricted to the analysis of a mixed suspension mixed product removal (MSMPR) crystallizer with both premixed and unpremixed feeds. The dimensionless exit age distribution of an MSMPR crystallizer is described by an exponentially decaying residence time distribution function.

In an IEM model formulation, a typical clump in a vessel is followed from its birth at the feed inlet. The clump or elementary volume is assumed to act as a batch vessel having uniform internal attributes like concentration and population density function and exchanging its contents with an arbitrary environment whose attributes are taken to be the mean attributes of all the clumps having the same residual lifetime in the vessel. The model assumes that micromixing is characterized by a single parameter termed *micromixing rate constant* (or sometimes *micromixing time constant*). For very small values of the micromixing rate constant (approaching zero), the reactive MSMPR crystallizer system is completely segregated and in a state of macrofluid, while for very large values (approaching infinity), the system behaves like a microfluid and the maximum mixedness limit is reached. Some interpretations have been attempted to relate the model parameter with those deduced from other theoretical considerations. The model description for a chemical reactor uses ordinary differential equations containing a single model parameter characterizing the micromixing effects. Thus, IEM models use a concept of external resistance to the segregated element and convective fluxes make the predominant contribution to mass transfer. Similar concepts will be used to describe the CSD of a precipitate resulting from chemical reaction between two components in a continuous crystallizer. Initially, the analytical treatment for the feeds that are mixed or become mixed immediately upon entering is developed and subsequently extended to the case of unpremixed feeds. The scope of this study is restricted to an MSMPR crystallizer configuration.

Model Formulation

For the present analytical treatment, a continuous crystallizer is considered with two feed streams, each containing a single species (Figure 1). These two species, A and B, react together homogeneously with first-order reaction kinetics with respect to each of reactants, component A being assumed limiting.

The reaction scheme considered is

$$A + B \rightarrow C \qquad r_c = kc_A c_B. \tag{1}$$

When the fluid phase becomes saturated with respect to C, precipitation of solid C from the liquid phase occurs simultaneously. Conventional power-law equations of the form

$$G = k_g \Delta c^g \tag{2}$$

and

$$B = k_b \Delta c^b = K_R G^i \tag{3}$$

are used to represent the growth and nucleation kinetics of the precipitation, respectively. Supersaturation, that is, the concentration driving force with respect to component C, is defined as the difference between the actual concentration and the solubility of component C in the solution phase. All the product in both solid and liquid phase, together with unreacted material, leaves the crystallizer through a single outlet.

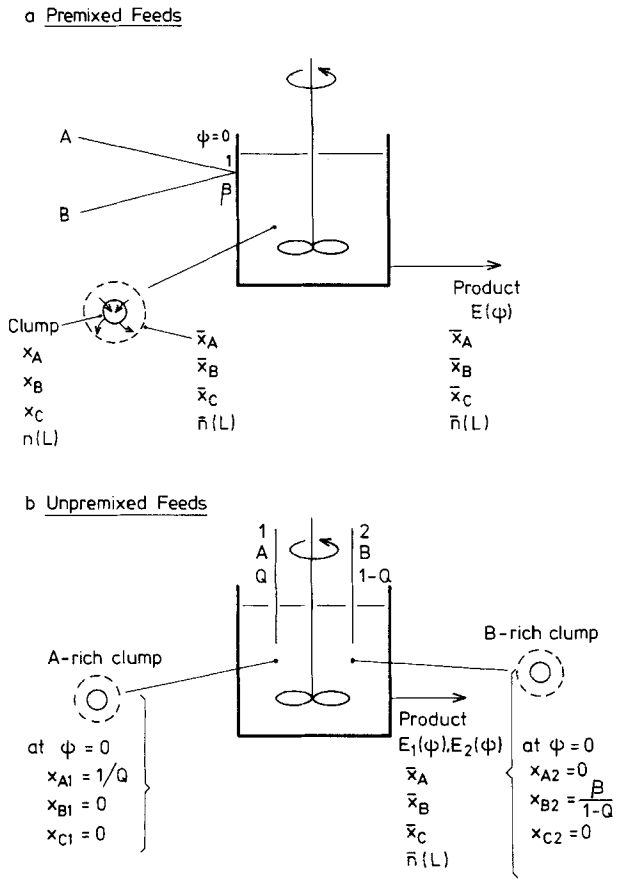

Figure 1. (a) Premixed feeds; (b) Unpremixed feeds.

Premixed feeds

The evaluation of the concentration profiles for the premixed feeds case of the present model follows lines similar to that for chemical reactors (Villermaux, 1981, 1986; David and Villermaux, 1983). If the following dimensionless variables are defined

$$x_A = \frac{c_A}{\bar{c}_{A_0}} \qquad x_B = \frac{c_B}{\bar{c}_{A_0}} \qquad x_C = \frac{c_C}{\bar{c}_{A_0}}$$

$$\gamma = k\bar{c}_{A_0}\tau \qquad \zeta = k_m\tau \qquad \beta = \frac{c_{B_0}}{\bar{c}_{A_0}}$$

$$\psi = \frac{t}{\tau} \qquad \alpha = \frac{1}{\bar{c}_{A_0}}\frac{dW}{d\psi} \qquad \xi = \theta - \psi,$$

the dimensionless concentration profiles in a clump of age ψ for A, B, and C in the fluid phase (Figure 1) may be written as

$$-\frac{dx_A}{d\psi} = \gamma x_A x_B + \zeta[x_A - \bar{x}_A(\xi)] \tag{4}$$

$$-\frac{dx_B}{d\psi} = \gamma x_A x_B + \zeta[x_B - \bar{x}_B(\xi)] \tag{5}$$

$$\frac{dx_C}{d\psi} = \gamma x_A x_B - \zeta(x_C - \bar{x}_C(\xi)) - \alpha, \tag{6}$$

where $\bar{x}_A(\xi)$, $\bar{x}_B(\xi)$, and $\bar{x}_C(\xi)$ are the average concentrations of all the clumps having residual lifetime ξ in the vessel. The boundary conditions are

$$x_A = 1 \qquad x_B = \beta \qquad x_C = 0 \qquad \text{at} \quad \psi = 0. \tag{7}$$

The mean concentrations of the components in the neighboring environment at a life expectancy ξ for an RTD function $E(\psi)$ and constant micromixing parameter ζ can be written as

$$\bar{x}_A(\xi) = \frac{1}{[1-F(\xi)]}\int_\xi^\infty x_A E(\psi)\,d\psi \tag{8}$$

$$\bar{x}_B(\xi) = \frac{1}{[1-F(\xi)]}\int_\xi^\infty x_B E(\psi)\,d\psi \tag{9}$$

$$\bar{x}_C(\xi) = \frac{1}{[1-F(\xi)]}\int_\xi^\infty x_C E(\psi)\,d\psi \tag{10}$$

where

$$F(\xi) = \int_0^\xi E(\psi)\,d\psi. \tag{11}$$

The specific case of RTD function, that is, exit age distribution, corresponding to a backmixed vessel or an MSMPR crystallizer is considered for the present study, and it is represented by

$$E(\theta) = \exp(-\theta). \tag{12}$$

For this exponentially decaying RTD function (Eq. 12), the life expectancy of a clump is zero. The attributes of all clumps in an MSMPR crystallizer are identical and equal to those of the exit stream.

The mean concentration of the components at the vessel outlet are the expected average values for all the clumps weighted by the RTD function and are therefore given by

$$\bar{x}_A = \int_0^\infty x_A \exp(-\psi)\,d\psi \tag{13}$$

$$\bar{x}_B = \int_0^\infty x_B \exp(-\psi)\,d\psi \tag{14}$$

$$\bar{x}_C = \int_0^\infty x_C \exp(-\psi)\,d\psi. \tag{15}$$

In order to facilitate an easy evaluation of the integrals in Eqs. 13–15, they can be conveniently transformed into differential equations as

$$\frac{d\hat{x}_A}{d\psi} = x_A \exp(-\psi) \tag{16}$$

$$\frac{d\hat{x}_B}{d\psi} = x_B \exp(-\psi) \tag{17}$$

$$\frac{d\hat{x}_C}{d\psi} = x_C \exp(-\psi) \tag{18}$$

with

$$\hat{x}_A = 0 \qquad \hat{x}_B = 0 \qquad \hat{x}_C = 0 \qquad \text{at} \quad \psi = 0 \tag{19}$$

as initial conditions. The values of $\hat{x}_A$, $\hat{x}_B$, and $\hat{x}_C$, determined by the integration of Eqs. 16–18 for $\psi \to \infty$, will equal $\bar{x}_A$, $\bar{x}_B$, and $\bar{x}_C$, respectively.

The population balance equation for such a clump with negligible attrition and agglomeration effects is

$$\frac{\partial n}{\partial \psi} + G\tau \frac{\partial n}{\partial L} = -\psi(n - \bar{n}) \tag{20}$$

with boundary conditions

$$n(0, \psi) = n^0 = B/G \tag{21}$$

$$n(L, 0) = 0. \tag{22}$$

The average population density $\bar{n}$ required in Eq. 20 may analogously be defined as

$$\bar{n}(L) = \int_0^\infty n(L, \psi) \exp(-\psi)\, d\psi. \tag{23}$$

The jth moment of the average product population density with respect to size is defined as

$$\bar{m}_j = \int_0^\infty \bar{n} L^j\, dL. \tag{24}$$

If the jth moment of population density in a clump with respect to size at any age ψ is defined as

$$\mu_j = \int_0^\infty n(L, \psi) L^j\, dL, \tag{25}$$

the moment transformation of Eq. 20 with respect to L yields

$$\frac{d\mu_0}{d\psi} = B\tau - \zeta(\mu_0 - \bar{m}_0) \tag{26}$$

$$\frac{d\mu_1}{d\psi} = \mu_0 G\tau - \zeta(\mu_1 - \bar{m}_1) \tag{27}$$

$$\frac{d\mu_2}{d\psi} = 2\mu_1 G\tau - \zeta(\mu_2 - \bar{m}_2) \tag{28}$$

$$\frac{d\mu_3}{d\psi} = 3\mu_2 G\tau - \zeta(\mu_3 - \bar{m}_3) \tag{29}$$

with boundary conditions

$$\mu_j = 0 \qquad \text{at} \quad \psi = 0. \tag{30}$$

The jth weighted mean moment $\bar{\lambda}_j$ of all clumps in the vessel may be defined as

$$\bar{\lambda}_j = \int_0^\infty \mu_j \exp(-\psi)\, d\psi \qquad j = 0, 1, 2, 3 \tag{31}$$

or alternatively evaluated from the differential equation as

$$\frac{d\hat{\lambda}_j}{d\psi} = \mu_j \exp(-\psi) \qquad j = 0, 1, 2, 3 \tag{32}$$

with the initial condition

$$\hat{\lambda}_j = 0 \qquad \text{at} \quad \psi = 0 \quad j = 0, 1, 2, 3. \tag{33}$$

Note that values of $\hat{\lambda}_j$ at $\psi \to \infty$ will equal $\bar{\lambda}_j$.

The variation of crystal size in a clump may be written as

$$\frac{dL}{d\psi} = G\tau \tag{34}$$

with $L = 0$ at $\psi = 0$ as the initial condition.

This set of equations describes completely the IEM model for a reactive precipitation system in a continuous MSMPR crystallizer with premixed feeds. The equations describing the concentration profiles for B (Eqs. 5, 9, 14, and in part, Eq. 7) may be redundant for the case of premixed feeds, as they may be determined in terms of those for component A. These are, however, included here for the sake of generality and are specifically required later for the case of unpremixed feeds.

Unpremixed feeds

Considerable attention has been devoted to the modeling of chemical reactors with separate feed streams, as the micromixing effects have been shown to be much more significant when the reactants enter separately than when these reactants are initially premixed before entry (Treleaven and Tobgy, 1971; Ritchie and Tobgy, 1978). When two streams, each containing one reactant, are fed separately to the vessel (Figure 1), the primary role of the interaction is to achieve a contact between the two reactive species in order for reaction and subsequent precipitation to occur. Conceptually, the same preceding model development should be applicable to each of the feed streams. Consequently, the same analytical description (Eqs. 4–6, 20–22, 24–30, 34) will be applicable to each of these streams, but the boundary conditions (Eq. 7) will be different. Assuming each of the feed streams contains only one reactant, the boundary conditions to equations describing concentration profiles, say, for stream 1 containing A alone, are

$$x_{A1} = \frac{1}{Q} \qquad x_{B1} = 0 \qquad x_{C1} = 0 \qquad \text{at } \psi = 0, \tag{35}$$

and then, for stream 2,

$$x_{A2} = 0 \qquad x_{B2} = \frac{\beta}{1 - Q} \qquad x_{C2} = 0 \qquad \text{at} \quad \psi = 0, \tag{36}$$

Table 1. Parameter Values Used in Model Calculations

Molecular weight of C, M_C, kg/kmol	100
Solubility of C, c^*, kmol/kg	0.001
Feed concentration of A, $\bar{c}_{A_0}$, kmol/kg	0.002
(note that both $\bar{c}_{A_0}$ and $\bar{c}_{B_0}$ are based on the total flow)	
$\beta\ (=\bar{c}_{B_0}/\bar{c}_{A_0})$	1.5
$\gamma\ (=k\bar{c}_{A_0}\tau)$	10
$\zeta\ (=k_m\tau)$	0.1, 1, 10
Fractional flow rate of A, Q	0.5
Crystal density of C, ρ_c, kg/m^3	2,660
Area shape factor	3.68
Volume shape factor	0.525
Mean residence time, τ, s	1,000
Nucleation order, b	3
Nucleation rate constant, k_b, number/[s·kg·(kmol/kg)^3]	1×10^{14}
Growth rate order, g	1.5
Growth rate constant, k_g, m/[s·(kmol/kg)$^{1.5}$]	0.2

where Q is the feed flow rate fraction. The RTDs for both these feed streams to an MSMPR crystallizer are represented by an exponentially decaying function (Eq. 12).

The mean exit concentrations of the components are

$$\bar{x}_A = \int_0^\infty [Qx_{A1} + (1-Q)x_{A2}]\exp(-\psi)\,d\psi \tag{37}$$

$$\bar{x}_B = \int_0^\infty [Qx_{B1} + (1-Q)x_{B2}]\exp(-\psi)\,d\psi \tag{38}$$

and

$$\bar{x}_C = \int_0^\infty [Qx_{C1} + (1-Q)x_{C2}]\exp(-\psi)\,d\psi. \tag{39}$$

The corresponding differential equations to evaluate the mean exit concentrations of all the clumps in the vessel are

$$\frac{d\hat{x}_A}{d\psi} = [Qx_{A1} + (1-Q)x_{A2}]\exp(-\psi) \tag{40}$$

$$\frac{d\hat{x}_B}{d\psi} = [Qx_{B1} + (1-Q)x_{B2}]\exp(-\psi) \tag{41}$$

$$\frac{d\hat{x}_C}{d\psi} = [Qx_{C1} + (1-Q)x_{C2}]\exp(-\psi) \tag{42}$$

with

$$\hat{x}_A = 0 \qquad \hat{x}_B = 0 \qquad \hat{x}_C = 0 \qquad \text{at} \quad \psi = 0 \tag{43}$$

as initial conditions.

Similarly, the weighted mean moments $\bar{\lambda}_j$ of all the clumps in the vessel may be evaluated from the differential equations as

$$\frac{d\hat{\lambda}_j}{d\psi} = [Q\mu_{j1} + (1-Q)\mu_{j2}]\exp(-\psi) \qquad j = 0,1,2,3 \tag{44}$$

with

$$\hat{\lambda}_j = 0 \qquad \text{at} \quad \psi = 0 \quad j = 0,1,2,3. \tag{45}$$

Equations 40–42 and 44 should be integrated until $\psi \to \infty$ to obtain the mean exit values.

The average population density at the vessel outlet may be determined as

$$\bar{n}(L) = \int_0^\infty [Qn_1(L,\psi) + (1-Q)n_2(L,\psi)]\exp(-\psi)\,d\psi. \tag{46}$$

Thus, two sets of equations (Eqs. 4–6, 20, 26–29, 32–34), each representing a clump from a stream, along with Eqs. 35–46, need to be considered simultaneously for this case. If the same RTD is used for both streams, the boundary condition (Eq. 21) to the population balance (Eq. 20) may be modified to

$$n(0,\psi) = n^0 = \left[Q\frac{B_1}{G_1} + (1-Q)\frac{B_2}{G_2}\right]. \tag{47}$$

The solution to Eq. 20 with Eqs. 22 and 47 as boundary conditions will represent the combined population density and Eq. 23 will then yield the mean product population density at the vessel exit. Thus, the use of the same RTD of both streams as represented by Eq. 12 simplifies the analysis.

Computational Aspects

In order to investigate the sensitivity of the parameters in the proposed model for a reactive precipitation system, the sets of equations described earlier were solved numerically for physicochemical conditions similar to those used in previous studies (Garside and Tavare, 1984, 1985). The specific set of relevant parameters used in the calculations is given in Table 1.

Premixed feeds

In the foregoing model description of an MSMPR crystallizer for the case of premixed feeds, it is assumed that the two feed streams mix completely in a clump just immediately after entry to the vessel, after which the clump is assumed notionally to preserve its segregation throughout the remainder of its stay within the vessel. The clump may be considered as an open system capable of exchanging mass with the surrounding environment whose attributes are assumed to be the mean of all clumps leaving the vessel for the present configuration.

For other RTD functions, the average attributes of all clumps at the same residual lifetime will constitute the environment attributes. Thus, each of these clumps acts as a small batch reactor exchanging matter with its surroundings. The configuration is represented by the set of 15 differential equations [Eqs. 4–6, 16–18, 26–29, 32, 34], but only 13 of them need to be solved simultaneously since the concentration profiles of A and B can be related by a simple algebraic equation.

At the start of the iterative algorithm, the mean values of 11 variables ($\bar{x}_A$, $\bar{x}_C$, $\bar{n}(L)$, $\bar{m}_j$, and $\bar{\lambda}_j$) were assumed as initial guesses and the set of 13 differential equations (Eqs. 4, 6, 16–18, 26–29, 32, 34), along with the partial differential equation (Eq. 20), solved simultaneously with appropriate

boundary conditions. The values evaluated from Eqs. 16, 18, 24, 32 at the end ($\psi \to \infty$) were compared with the assumed guesses. An arbitrary convergence limit of 1% relative error based on the assumed guess was set. If the calculated relative error in any of the assumed guesses was above the convergence limit, the newly determined mean values of variables at the vessel exit were then used as guesses for the subsequent iteration.

Just after the entry, only reaction occurs initially in each of these clumps until the concentration of product C reaches its saturation point. As soon as the clump becomes supersaturated with respect to C, nucleation and subsequent evolution of the particle size distribution via growth commences. Consequently, only those differential equations describing the concentration profiles (Eqs. 4, 6, 16, 18) were integrated initially (α having set equal to zero) until the concentration of C in the liquid phase reached the saturation concentration. Once the reaction mixture of the clump became supersaturated with respect to C, the set of 13 differential equations, along with the partial differential equation describing the population balance in a clump and the integrals (Eqs. 23, 24) evaluating the average population density and its first four moments at the vessel exit, were solved simultaneously. Note that α was evaluated on the basis of mass deposited on the crystal surface area in a clump.

All the differential equations involved were integrated by the fourth-order Runge–Kutta method with an integration step length of $\Delta\psi = 0.0005$ using appropriate initial conditions. The partial differential equation (Eq. 20) was solved by the modified method of numerical integration along the characteristics with a specified grid length of crystal size. The initial guesses of $\bar{n}(L)$ required in Eq. 20 were set equal to zero at all grids and the integral in Eq. 23 was evaluated numerically using the Euler method. In the algorithm, the set of 13 differential equations was initially integrated with a step length of $\Delta\psi = 0.0005$ until the increment in size was equal to the grid length of crystal size used (2 μm) in the solution of the partial differential equation. The growth rate and nuclei population density were defined at the end of grid, and the solution of the partial differential equation moved forward by the time required to increase the crystal size by one grid length (2 μm). The step length for the age to evaluate the integral in Eq. 23 was also the same, that is, the time required to increase the crystal size by one grid length. If occasionally the step length of $\Delta\psi = 0.0005$ proved too large and produced a size increment greater than one grid on the crystal size axis, then the step length of age ($\Delta\psi$) for those steps was reduced proportionately in order to keep the increment below the normal step length of 2 μm.

Unpremixed feeds

For the case of unpremixed feeds, two streams, each containing one reactant, are assumed to enter separately and may have their own RTDs. As the same description of the previous case is applicable to each of these streams, the algorithm is rather similar but still further complicated. The same RTD for both streams was considered in the subsequent analysis and the combined population density (Eqs. 20, 22, and 47) evaluated using the numerical technique as described in the preceding section. Two sets of equations depicting A-rich and B-rich clumps with different boundary conditions need to be solved simultaneously along with the set of differential equations describing the average attributes of all the clumps present in the vessel. Thus, instead of a set of 13 differential equations in the case of premixed feed, 23 differential equations (Eqs. 4–6, 26–29, 34 for each A- and B-rich clumps, 40–42, 44) need to be solved simultaneously. Similar procedure and convergence limits were used in this case for the iterative technique.

Results and Discussion

Using the physicochemical parameters listed in Table 1, calculations were performed to evaluate the crystallizer performance as predicted by the two cases of the IEM model (Figure 1).

The variations of average dimensionless concentrations of the limiting reactant A, $\hat{x}_A$, and product C, $\hat{x}_C$, as defined by Eqs. 16 and 18 for the case of premixed feeds and by Eqs. 40 and 42 for the case of unpremixed feeds, respectively, were evaluated numerically. All species concentration profiles showed a monotonous increase with ψ due to the integration process involved in their evaluations. These profiles were similar to the corresponding variations for the completely segregated system ($\zeta = 0$, *CS* (II) Model II) reported previously by Garside and Tavare (1985) and indicated that an upper limit of $\psi = 10$ was satisfactory for the evaluations of the integrals (Eqs. 13–15, 37–39). The values of $\hat{x}_A$ and $\hat{x}_C$ evaluated at $\psi = 10$ therefore represented the average of the respective dimensionless concentrations $\bar{x}_A$ and $\bar{x}_C$ at the exit of an MSMPR crystallizer under the assumptions of the IEM model. The concentration profiles for the case of premixed feeds were generally closer to those of a completely segregated system (*CS* (II), Model II, Garside and Tavare, 1985), but substantially different for the case of unpremixed feeds.

The resulting crystal-size distributions as illustrated by the conventional population density plots for the two cases are shown in Figure 2. Also reproduced in Figure 2 for comparison purposes are the population density plots for the extremes of micromixing, viz., maximum mixedness (Model I), *MM*(I) and complete segregation (Model II), *CS*(II), and the two environment model with premixed feeds from the previous studies (Garside and Tavare, 1985; Tavare, 1992). Corresponding details of size distribution statistics are included in Table 2. Clearly both the reaction and crystallization performance characteristics for the case of premixed feeds for low ζ lie within those for the limiting cases of micromixing. The model description used to characterize the micromixing effect for this case is akin to that of the completely segregated case and utilizes an additional step of first-order mass exchange with the surrounding environment having the same residual lifetime. Consequently, with an increase in micromixing parameter ζ, the performance characteristics should move away from those of the completely segregated case and toward those of the maximum mixedness case. The calculated performance characteristics for product C both in the solution and in the solid phase appear not to reflect this trend. With an increase in ζ, the relative contributions of terms associated with their description change; this appears to influence the attributes of a clump and hence the average product characteristics at the outlet of the crystallizer. For

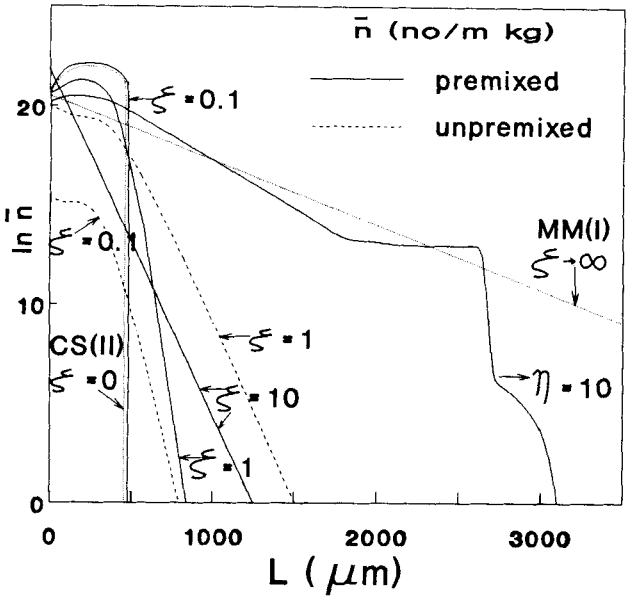

Figure 2. Product population density plots (data as Table 1).

high values of ζ, the calculated average concentration of product C at the exit is higher than that for the case of maximum mixedness (Model I, *MM*(I)). Thus, the crystallizer operates at high average solution concentration and consequently low magma concentration of product C, yielding different product characteristics from those of the maximum mixedness case (Model I, *MM*(I)).

For the case of unpremixed feeds, micromixing parameter ζ has significant influence on the reaction and subsequent crystallization, as can be seen from Figure 2. With an increase in ζ, a greater interaction by exchanging material between the clumps results in higher conversion of A and production of solid phase C. The peculiar shapes of population density curves for this case in Figure 2 demonstrate the enormous mixing contribution to the overall crystallizer behavior and bear some similarity with those reported previously; for example, ammonium sulfate (Tavare, 1989) and sodium chloride population density plots from a pilot-plant crystallizer (Grootscholten et al., 1981, 1982). At low values of ζ, the plots have different shapes, showing strong segregation effects. At $\zeta = 10$, the population density curves and their corresponding product statistics are, however, similar for premixed and unpremixed feed conditions. With an increase in ζ, the relative contributions of the terms in the model equation change; they appear to influence the attributes of a clump and hence the average product characteristics at the outlet of a crystallizer. For the two-environment model, with an increase in its micromixing parameter η there appears to be a gradual movement of both the reaction and crystallization performance characteristics from the completely segregated to the maximum mixedness case (Tavare, 1992). The population density plot for $\eta = 10$ in Figure 2 approaches that of the maximum mixedness case.

In the two-environment model formulation, the vessel is divided into two environments, the entering environment, where the fluid elements are completely segregated, and the leaving environment, which is always in the state of maximum mixedness. Material transfer from the entering environment is assumed to take place at a rate proportional to the amount of material remaining in the entering environment and with a specific rate of transfer parameter used as a micromixing parameter of the model. When this micromixing parameter is zero, there is no transfer from the entering to the leaving environment and the whole vessel is completely segregated. When this parameter is infinitely large, the entire entering material is immediately transferred into the leaving environment so that the vessel is in the state of maximum mixedness.

Effect of Damköhler number γ

The influence of the reaction rate constant k upon the crystallization characteristics can be explored by examining the effect of changes in the dimensionless reaction group γ (the Damköhler number). This reaction group characterizes the reaction performance, and hence determines the dimensionless concentration of A, $\bar{x}_A$, for a given micromixing parameter ζ. Keeping all other parameters in Table 1 constant, γ was varied over the range 0.1 to 1,000, thus covering a 10^4-fold range of γ for a given ζ. Figures 3 and 4 show the results of these calculations.

Figure 3 shows the variations of $\bar{x}_A$ and $\bar{x}_C$ with γ at different levels of ζ for the two cases, viz., premixed and unpremixed feeds. Also included in Figure 3 are those varia-

Table 2. Performance Characteristics of the IEM Micromixing Model*

Case	ζ or η	$\bar{x}_A$	$\bar{x}_C$	$\bar{L}_w$, μm	CV_w, %	$N_T \times 10^{-6}$, No./kg
MM(I)	∞	0.136	0.567	930	50.0	0.24
CS(II)	0	0.096	0.540	353	22.5	1.20
IEM:						
Premixed	0.1	0.096	0.541	352	22.2	1.55
	1.0	0.100	0.549	343	24.1	0.7
	10.0	0.117	0.628	349	48.9	0.22
IEM:						
Unpremixed	0.1	0.891	0.108	451	27.6	0.0013
	1.0	0.459	0.401	488	34.1	0.15
	10.0	0.166	0.601	348	48.8	0.19
Environment:						
Premixed	10.0	0.111	0.545	958	57.9	0.40

*$\gamma = 10$; Figures 2

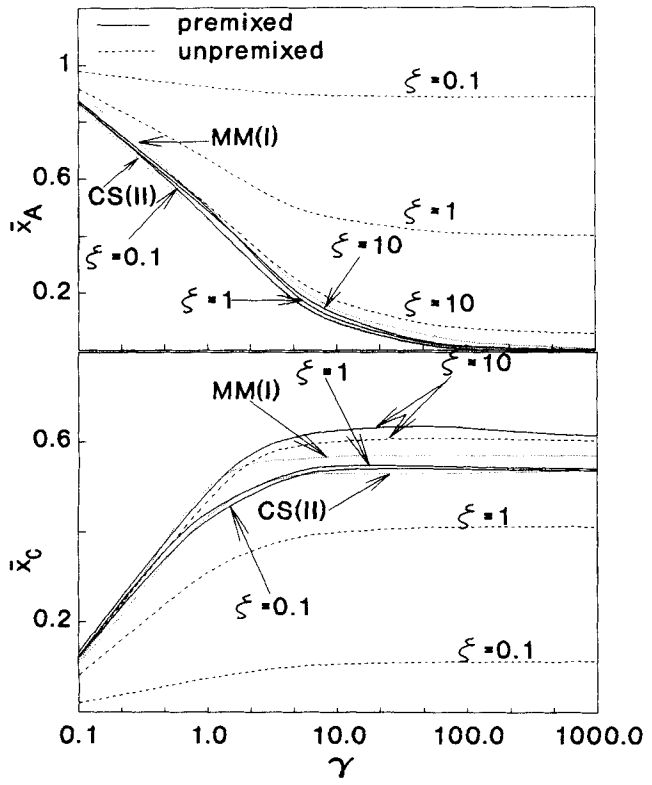

Figure 3. Effect of Damköhler number, γ, on outlet concentration profiles of *A* and *C*.

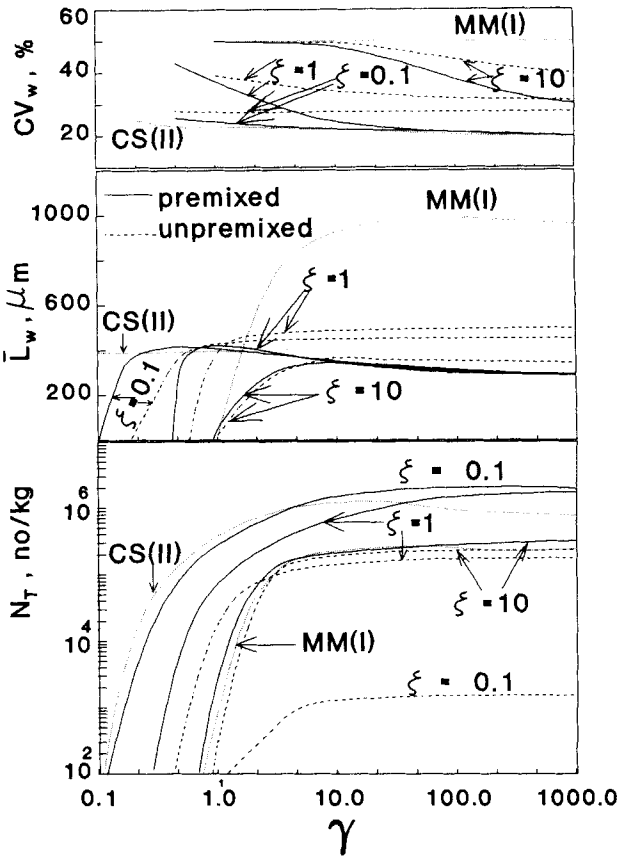

Figure 4. Effect of Damköhler number, γ, on product characteristics.

tions for extremes of micromixing levels. Low values of γ result in lower reaction rates and yield lower conversion. With an increase in γ, $\bar{x}_A$ decreases; $\bar{x}_C$ increases rapidly at lower γ and then remains almost constant as a consequence of producing solid C. The concentration profile of A with γ for the case of premixed feeds lies within the range of concentration profiles for the extremes of micromixing. Although the concentration profile of A follows a correct trend, it is less sensitive to micromixing parameter ζ. Significant influence of the micromixing parameter ζ on the performance characteristics for the case of unpremixed feeds, however, is apparent in Figure 3. Similar variations of $\bar{x}_A$ have been reported previously for the study of the simple reaction only (Villermaux, 1981; Villermaux and David, 1983). At $\zeta = 10$, the calculated concentration profiles of C with γ for both the premixed and unpremixed cases, particularly at high γ, lie outside the range of concentration profiles for the extremes of micromixing. For the case of the two-environment model with premixed feeds, the calculated concentration profiles of both A and C with γ, however, lie within the bounds for the extreme micromixing levels.

Crystallization performance characteristics, viz., weight mean size, coefficient of variation, and specific total number of crystals per unit of solvent mass, are depicted in Figure 4. The weight mean product size increases rapidly at lower γ (< 2) above a certain critical γ for both the cases. The critical γ at which the solid product C starts appearing depends on the micromixing parameter. With an increase in ζ, the critical γ increases for both these cases; usually it is lower for the case of premixed than for unpremixed feeds. For the same ζ at lower γ (< 2), the rate of increase in weight mean size for premixed feeds is higher than that for unpremixed feeds, the difference in rates for these two feed conditions reducing with an increase in ζ. At higher $\gamma (> 2)$, the weight mean size decreases slowly with γ for the case of premixed feeds while it increases for the other case. Usually the weight mean size for premixed feeds is lower than that for unpremixed feeds. In the case of the two-environment model, the weight mean size passes through a peak showing rather wider variation. The coefficient of variation based on the weight distribution appears insensitive to γ, apart from a slight decrease for large γ at $\zeta = 10$. For a given γ at any ζ, the coefficient of variation for premixed feeds is lower than that for unpremixed feeds. There appears to be some trend in the variation of CV_w with ζ and the range of CV_w for the extremes of micromixing provides the bounds for intermediate levels of micromixing. For both the two-environment and IEM models, the coefficient of variation based on weight distribution decreases with γ. It may provide a better, though less sensitive, indicator.

The specific total number increases rapidly at lower $\gamma (< 2)$ just above the critical γ and slowly at higher $\gamma (> 2)$. The variation of N_T with γ for intermediate levels of micromixing is not exactly bounded between that for the two micromixing extremities, but there is a trend with ζ. For premixed feeds, with an increase in ζ the curve representing the variation moves away from the complete segregation to the maximum mixedness case. For the case of the two-environment model with premixed feeds, there appears to be a similar trend in

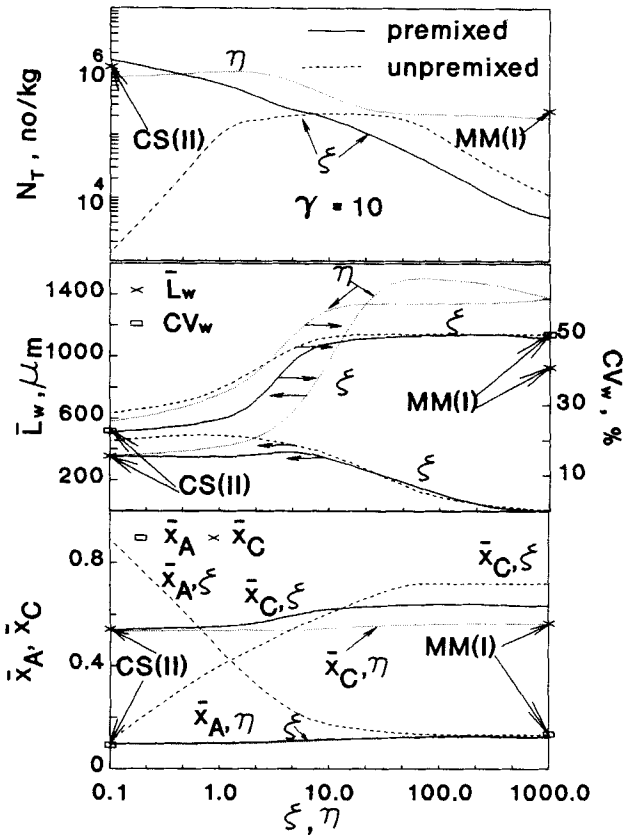

Figure 5. Effect of micromixing parameter, ζ, on product characteristics.

the variation at low γ while it is reversed at high γ, the system being nearer to segregation. In the case of unpremixed feeds for the present model, the curves appear to approach the maximum case from the opposite side. Thus, at large ζ, the crystallizer operates at near maximum mixedness level in both these feed cases.

Effect of micromixing parameter ζ

Keeping all other parameters in Table 1 constant, the micromixing parameter was varied from 0.1 to 1,000, thus covering the 10^4-fold range. The results of these calculations depicting the effect of micromixing parameter ζ on the performance characteristics of both reaction and crystallization in both premixed and unpremixed feeds for $\gamma = 10$ are reported in Figure 5. Also shown in Figure 5 are those values for the extreme micromixing levels and their variations with micromixing parameter η for the two-environment model.

The calculated dimensionless species concentrations, $\bar{x}_A$ and $\bar{x}_C$, at the extreme micromixing levels only slightly differ and appear insensitive to the micromixing parameters over the entire range. The calculated dimensionless concentration profile for species A, $\bar{x}_A$, in both models lies within the small range of its values at the extreme micromixing levels, while the calculated concentrations for C lie within the bounds for small ζ and all η, but at high ζ they exceed the bound of the maximum mixedness case. For high values of ζ, the calculated average concentration of product C at the exit is higher than that for the case of maximum mixedness (Model I, *MM*(I)). The crystallizer operates at high average solution concentration of component C, and consequently at low magma concentration of product C, yielding different product characteristics from those of the maximum mixedness case (Model I, *MM*(I)). In the case of unpremixed feeds, with an increase in ζ, $\bar{x}_A$ decreases and $\bar{x}_C$ increases rapidly at high ζ up to $\zeta = 10$ and they both remain almost constant over the rest of the ζ range investigated.

Crystallization performance characteristics, however, show substantial changes. The product weight mean size is almost constant over low ζ and then passes through a slight maximum, decreasing rapidly with an increase in ζ for both premixed and unpremixed feeds. The variation of the weight mean size with η shows a sigmoidal curve with the point of inflection at about $\eta = 10$. At higher micromixing parameters, it exceeds the range of the extreme micromixing values for both models. In the case of IEM model, it is lower than the lower bound, probably due to higher exit solution concentration of species C, while in the case of the environment model, it is higher than the higher bound, perhaps due to the feeding of slurry from the entering environment to the leaving environment, operating at a higher level of supersaturation. The specific total crystal number decreases with ζ for premixed feeds, and for unpremixed feeds it initially shows a rapid increase, then remains constant, and finally shows a slow decrease with ζ, while its variation with η shows a sigmoidal curve showing a rapid decrease over the most sensitive range of η. The coefficient of variation increases with ζ for both premixed and unpremixed feeds lies within the range of CV_w for extreme micromixing limits and it is generally lower for premixed feeds. The variations of the coefficient of variation with the micromixing parameters show sigmoidal curves with the point of inflection at micromixing parameters of around 4–5. The variation of the coefficient of variation for the two-environment model, however, exceeds the range of values for extremes of micromixing. In general, the performance characteristics for unpremixed feeds are more sensitive to the variation of ζ than those for premixed feeds. Although the direct comparison with the study of Pohorecki and Baldyga (1979) is difficult due to different physicochemical parameters used, the trends in the variation of performance characteristics with the micromixing parameters over the small range are similar.

Effect of feed conditions (Q and β)

Finally, the effect of feed conditions was explored by changing the fractional flow rate, Q, and dimensionless inlet concentration of B, β, independently. Keeping all other parameters in Table 1 constant, Q was varied, the results being shown in Figure 6 for two micromixing parameters ($\zeta = 0.1$ and 1.0). $\bar{x}_A$ increases linearly with Q up to $Q = 0.5$, and a slow subsequent increase in $\bar{x}_A$ is observed with further increases in Q. $\bar{x}_C$ passes through a maximum at $Q = 0.5$. For a given Q, with an increase in micromixing parameter, ζ, $\bar{x}_A$ decreases and consequently $\bar{x}_C$ increases. It can be seen from Figure 6 that no solid C is produced for $Q > \sim 0.72$ at $\zeta = 0.1$ and $Q > \sim 0.82$ at $\zeta = 1.0$. Perhaps $Q = 0.5$ appears to be a satisfactory choice for the operation of a crystallizer with unpremixed feeds.

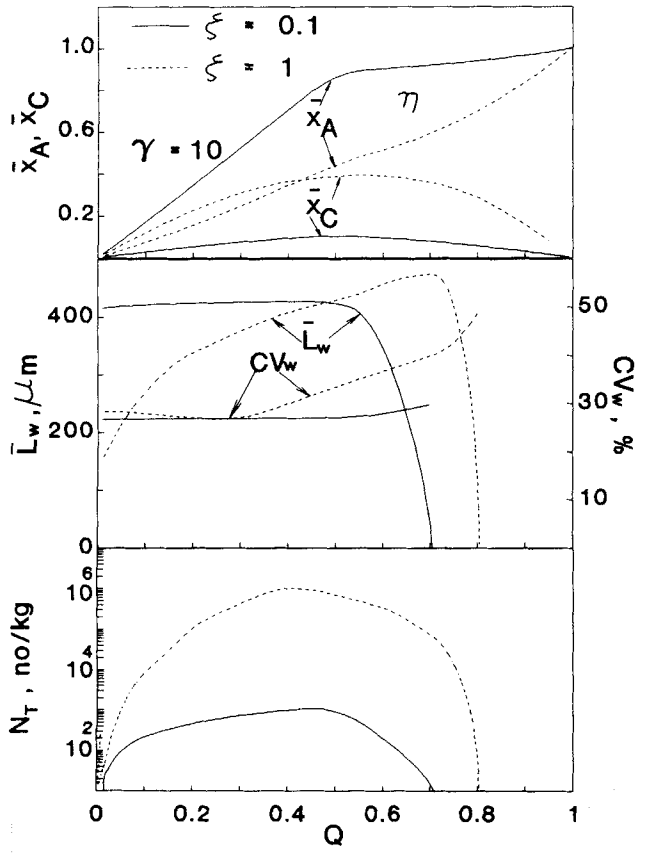

Figure 6. Effect of fractional flow rate, Q, on the crystallizer performance.

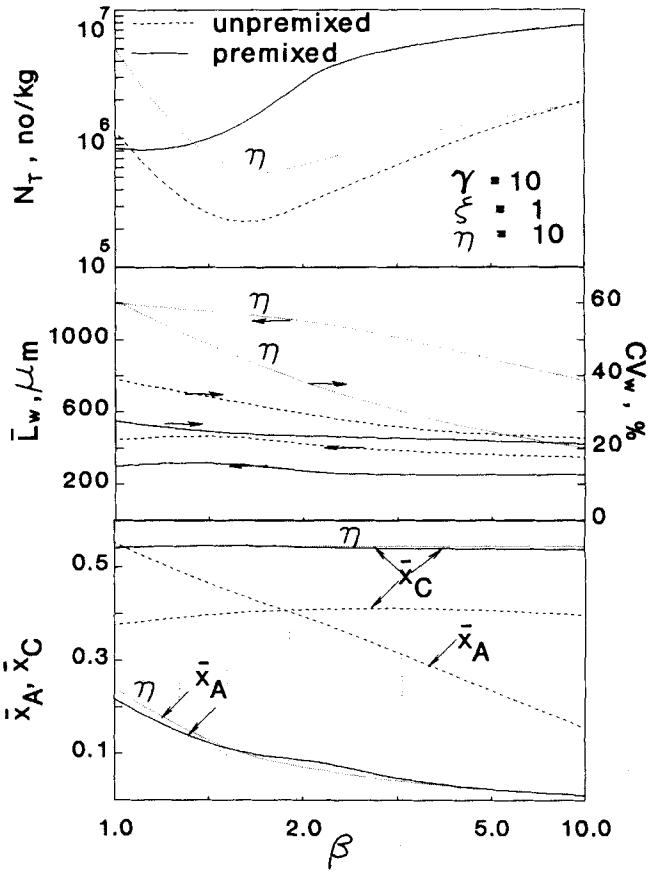

Figure 7. Effect of dimensionless inlet concentration of B, β, on the crystallizer performance.

The product weight mean size remains almost constant up to $Q \sim 0.6$ and then decreases rapidly with a further increase in Q for $\zeta = 0.1$. For $\zeta = 1.0$, it increases slowly, however, until $Q \sim 0.75$, and then decreases rapidly. The specific total crystal number similarly passes through a maximum, having larger values at $\zeta = 1.0$ than that at $\zeta = 0.1$. The coefficient of variation increases with Q at a slightly faster rate for $\zeta = 1$ than that for $\zeta = 0.1$.

Keeping all other quantities constant, the dimensionless feed concentration of B, β, was varied over the range of 1 to 10. The results of calculations for $\zeta = 1.0$ in both cases of the model are presented in Figure 7. $\bar{x}_A$ decreases and $\bar{x}_C$ increases slowly due to increased reaction rate with an increase in β for both cases. For premixed feeds, at any β, $\bar{x}_A$ is lower and $\bar{x}_C$ higher than those for unpremixed feeds. With an increase in β, the weight mean size passes through a slight maximum, the specific total number of crystals increases after passing through a minimum, and the coefficient of variation decreases slowly for both cases; a larger weight mean size with lower specific number of crystals and slightly higher coefficient of variation is calculated for unpremixed feeds than the corresponding results for premixed feeds at any β. For the two-environment model with an increase in β, most results for premixed feeds appear to show variation similar to those of the IEM model.

Investigated in the foregoing analysis are the effects of several parameters (γ, ζ, Q, β) on the reaction and crystallization performance of a reactive precipitation process and several others, such as crystallization kinetics, residence time distribution, and operating conditions, may have significant influence. In order to evaluate the performance characteristics for RTD functions other than the exponentially decaying relation employed for an MSMPR crystallizer, the attributes of the environment surrounding the clump are represented by the average of all the clumps having the same residual lifetime. This analysis is concerned with a global characterization of the performance characteristics of a reactive precipitation system in a continuous crystallizer. Local characterization may perhaps provide valuable information regarding the micromixing process.

David and Villermaux (1983) in their review provided a link between the systems approach of the IEM model and the fluid mechanics approach in the framework of the turbulence theory. They assumed that micromixing proceeds via three main mechanisms relying on the concept of fluid aggregates or clumps, viz., laminar stretching, turbulent erosion, and molecular diffusion, each being represented by a characteristic time constant. These time constants can be estimated from the semiempirical correlations (see also, for example, Mehta and Tarbell, 1983, 1987). The micromixing parameter ζ of the IEM micromixing model can be equivalent to one-half of the micromixing parameter η of the two-environment micromixing model (Ng and Rippin, 1965). Although a relationship between the mechanistic and direct turbulence models has been established, the detailed numerical analysis might

predict very different performance characteristics for complex reactions having different intrinsic timescales than the turbulent micromixing timescale (Chang et al., 1986; Mehta and Tarbell, 1987). While proposing the master micromixing model and technique for its parameter estimation from experimental responses, Call and Kadlec (1989) pointed out that one of the difficulties associated with the application of the mathematical models in industrial practice was to estimate reliable micromixing parameters.

The analysis presented here lays no claim to providing a detailed physical insight into the interaction of mixing, reaction, and subsequent crystallization, but rather provides a means of evaluating and subsequently predicting the performance for a given crystallizer configuration. The basis of the general technique is the use of a known reactive crystallization system to evaluate the parameters of a model that represents by simulation the performance obtained experimentally from the crystallizer. A complete set of experimental data and a powerful parameter characterization technique are required to determine the model parameters and subsequently relate them to the crystallizer hydrodynamics. Generally, the micromixing effects are much more important when the reactants enter separately than when they are initially premixed just before entry.

Acknowledgment

The author is indebted to Professors J. Villermaux and R. Pohorecki for their valuable and constructive reviews on the original manuscript.

Notation

b = nucleation order
B = nucleation rate, number/s·kg solvent
c = concentration, kmol/kg
c^* = saturation concentration, kmol/kg
Δc = concentration driving force, kmol/kg
g = growth rate order
G = linear growth rate, m/s
i = relative kinetic order (= b/g)
k_a = area shape factors
k_b = nucleation rate constant, number/[s·kg·(kmol/kg)^b]
k_g = growth rate constant, m/[s·kg·(kmol/kg)^g]
k_m = micromixing rate constant, L/s
K_R = relative rate constant, number/[s^{i-1}·m^i·kg]
L = crystal size, m
m_j = jth moment of product population density (Eq. 24), number ·m^j/kg
M_C = molecular weight of C
n^0 = nuclei population density, number/m·kg
N_T = crystal number concentration, number/kg
r_C = reaction rate, kmol/s·kg
t = time, age, s
W = instantaneous crystal mass in a clump, kmol/kg

Greek letters

α = dimensionless solid deposition rate
θ = dimensionless residence time ($\theta = t/\tau$)
μ_j = jth moment of population density (Eq. 25), number·m^j/kg
ρ_c = crystal density, kg/m^3
τ = mean residence time, s

Subscripts

w = weight basis
1,2 = inlet streams

Literature Cited

Aslund, B. L., and A. C. Rasmuson, "Semibatch Reaction Crystallization of Benzoic Acid," *AIChE J.*, **38**, 328 (1992).

Baldyga, J., "Micromixing and Precipitation," in *Proc. of the 12th Symp. on Industrial Crystallization*, Vol. 1, Z. H. Rojkowski, ed., Warsaw, Poland, p. 2-003 (1993).

Baldyga, J., and R. Pohorecki, "The Effect of Micromixing on the Precipitation Process in a Premixed Feed Continuous Stirred Tank Crystallizer (CSTC)," Conf. on Mixing Colloque d' Agitation Mécanique, ENSIGC, Toulouse, France (1986).

Baldyga, J., R. Pohorecki, W. Podgorska, and B. Marcant, "Micromixing Effects in Semibatch Precipitation," *Industrial Crystallization*, A. Mersmann, ed., Garmisch-Partenkirchen, Germany, p. 175 (1990).

Becker, G. W., Jr., and M. A. Larson, "Mixing Effects in Continuous Crystallization," *Chem. Eng. Prog. Symp. Ser. No. 95*, **65**, 14 (1969).

Call, M. L., and R. H. Kadlec, "Estimation of Micromixing Parameters from Tracer Concentration Fluctuation Measurements," *Chem. Eng. Sci.*, **44**, 1377 (1989).

Chang, L.-J., R. V. Mehta, and J. M. Tarbell, "An Evaluation of Models of Mixing and Chemical Reaction with a Turbulence Analogy," *Chem. Eng. Commun.*, **42**, 139 (1986).

Costa, P., and C. Trevissoi, "Some Kinetic and Thermodynamic Features of Reactions Between Partially Segregated Fluids," *Chem. Eng. Sci.*, **27**, 653 (1972a).

Costa, P., and C. Trevissoi, "Reactions with Nonlinear Kinetics in Partially Segregated Fluids," *Chem. Eng. Sci.*, **27**, 2041 (1972b).

Danckwerts, P. V., "The Effects of Incomplete Mixing on Homogeneous Reactions," *Chem. Eng. Sci.*, **8**, 93 (1958).

David, R., and J. Villermaux, "Micromixing Effects on Complex Reactions in a CSTR," *Chem. Eng. Sci.*, **30**, 1309 (1975).

David, R., and J. Villermaux, "Recent Advances in the Understanding of Micromixing Phenomena in Stirred Reactors," *Chem. Eng. Commun.*, **21**, 105 (1983).

Fitchett, D. E., and J. M. Tarbell, "Effect of Mixing on the Precipitation of Barium Sulphate in an MSMPR Reactor," *AIChE J.*, **36**, 511 (1990).

Garside, J., and N. S. Tavare, "Mixing, Reaction, and Precipitation in an MSMPR Crystallizer: Effects of Reaction Kinetics on the Limits of Micromixing," *Industrial Crystallization 84*, S. J. Jancic and E. J. de Jong, eds., Elsevier, Amsterdam, p. 131 (1984).

Garside, J., and N. S. Tavare, "Mixing, Reaction, and Precipitation: Limits of Micromixing in an MSMPR Crystallizer," *Chem. Eng. Sci.*, **40**, 1485 (1985).

Grootscholten, P. A. M., E. J. de Jong, and A. Scrutton, "Chemical Engineering Approach to Industrial Crystallization," *Proc. World Cong. Chem. Eng. IV*, Montreal, p. 59 (1981).

Grootscholten, P. A. M., C. J. Asselbergs, A. Scrutton and E. J. de Jong, "Effect of Crystallizer Geometry on Crystallizer Performance," *Industrial Crystallization 81*, S. J. Jancic and E. J. de Jong, eds., North Holland, Amsterdam, p. 189 (1982).

Harada, M., K. Arima, W. Eguchi, and S. Nagata, "Micromixing in a Continuous Flow Reactor (Coalescence and Redispersion Model), *The Memoirs of the Faculty of Engineering*, Vol. 24, Kyoto Univ., Kyoto, Japan, p. 431 (1962).

Iyer, H. V., and T. M. Przybycien, "Protein Precipitation: Effects of Mixing on Protein Solubility," *AIChE J.*, **40**, 349 (1994).

Klein, J. P., R. David, and J. Villermaux, "Interpretation of Experimental Liquid Phase Micromixing Phenomena in a Continuous Stirred Reactor with Short Residence Times," *Ind. Eng. Chem. Fundam.*, **19**, 373 (1980).

Kuboi, R., M. Harada, J. M. Winterbottom, A. J. S. Anderson, and A. W. Nienow, "Mixing Effects in Double-Jet and Single-Jet Precipitation," *Proc. World Cong. III of Chem. Eng.*, Paper 8g-302, Tokyo, Sept., p. 1040 (1986).

Marcant, B., and R. David, "Experimental Evidence for and Prediction of Micromixing Effects in Precipitation," *AIChE J.*, **37**, 1698 (1991).

Marcant, B., and R. David, "Influence of Micromixing on Precipitation in Several Crystallizer Configurations," *Proc. of the 12th Symp. on Industrial Crystallization*, Vol. 1, Z. H. Rojkowski, ed., Warsaw, Poland, p. 2-021 (1993).

Marcant, B., and R. David, "Prediction of Micromixing Effects in

Precipitation: Case of Double-Jet Precipitators," *AIChE J.*, **40**, 424 (1994).
Mehta, R. V., and J. M. Tarbell, "Four Environment Model of Mixing and Chemical Reaction. I: Model Development," *AIChE J.*, **29**, 320 (1983).
Mehta, R. V., and J. M. Tarbell, "An Experimental Study of the Effect of Turbulent Mixing on the Selectivity of Competing Reactions," *AIChE J.*, **33**, 1089 (1987).
Mydlarz, J., J. Reber, D. Briedis, and J. A. Voigt, "Kinetics of Zinc Oxalate Precipitation in a Mininucleator—MSMPR Crystallizer System," *AIChE Symp. Ser. No. 284*, **87**, 158 (1990).
Ng, D. Y. C., and D. W. T. Rippin, "The Effect of Incomplete Mixing on Conversion in Homogeneous Reactions, *Proc. Euro. Symp. on Chemical Reaction Engineering*, Pergamon Press, Oxford, p. 161 (1965).
Plasari, E., R. David, and J. Villermaux, "Micromixing Phenomena in Continuous Stirred Reactors Using a Michaelis-Menton Reaction in Liquid Phase," *ACS Symp. Ser. 65, Chem. Reaction Eng.*, Houston, p. 125 (1978).
Podgorska, W., J. Baldyga, and R. Pohorecki, "Micromixing Effects in Double Feed Semibatch Precipitation," *Proc. Symp. on Industrial Crystallization*, Vol. 1, Z. H. Rojkowski, ed., Warsaw, Poland, p. 2-015 (1993).
Pohorecki, R., and J. Baldyga, "The Influence of Intensity of Mixing on the Rate of Precipitation," *Industrial Crystallization 78*, E. J. de Jong and S. J. Jancic, eds., North-Holland, Amsterdam, p. 249 (1979).
Pohorecki, R., and J. Baldyga, "The Use of a New Model of Micromixing for Determination of Crystal Size in Precipitation," *Chem. Eng. Sci.*, **38**, 79 (1983a).
Pohorecki, R., and J. Baldyga, "New Model of Micromixing in Chemical Reactors: 1. General Development and Application to a Tubular Reactor," *Ind. Eng. Chem. Fundam.*, **22**, 392 (1983b).
Pohorecki, R., and J. Baldyga, "New Model of Micromixing in Chemical Reactors: 2. Application to a Stirred Tank Reactor," *Ind. Eng. Chem. Fundam.*, **22**, 398 (1983c).
Pohorecki, R., and J. Baldyga, "The Effects of Micromixing and the Manner of Reactor Feeding on Precipitation in Stirred Tank Reactors," *Chem. Eng. Sci.*, **43**, 1949 (1988).
Ritchie, B. W. and A. H. Togby, "General Population Balance Modeling of Unpremixed Feed Streams Chemical Reactors: A Review," *Chem. Eng. Commun.*, **2**, 249 (1978).
Tavare, N. S., "Mixing in Continuous Crystallizers," *AIChE J.*, **32**, 705 (1986).
Tavare, N. S., "Micromixing Limits in an MSMPR Crystallizer," *Chem. Eng. Technol.*, **12**, 1 (1989).
Tavare, N. S., "Mixing, Reaction and Precipitation: Environment Micromixing Models in Continuous Crystallizers: I. Premixed Feeds," *Comput. Chem. Eng.*, **16**, 923 (1992).
Tavare, N. S., "Mixing, Reaction and Precipitation: Micromixing Models in Continuous Crystallizers," *Proc. Symp. on Industrial Crystallization*, Vol. 1, Z. H. Rojkowski, ed., Warsaw, Poland, p. 2-073 (1993).
Tosun, G., "An Experimental Study of the Effects of Mixing Intensity on Particle Size Distribution in Barium Sulphate Precipitation," *Proc. Euro. Conf. on Mixing*, Pavia, p. 161 (May, 1988).
Tovistiga, G., and H.-P. Wirges, "The Effect of Mixing Intensity on Precipitation in a Stirred Tank Reactor," *Industrial Crystallization '90*, A. Mersmann, ed., Garmisch-Partenkirchen, Germany, p. 169 (1990).
Treleaven, C. P., and A. H. Togby, "Conversion in Reactors Having Separate Reactant Feed Streams. The State of Maximum Mixedness," *Chem. Eng. Sci.*, **26**, 1259 (1971).
Villermaux, J., "Drop Break-Up and Coalescence: Micromixing Effects in Liquid-Liquid Reactors," *Multiphase Chemical Reactors*, Vol. I, Fundamentals, A. E. Rodrigues, J. M. Calo, and N. H. Sweed, eds., NATO Advanced Study Institute Ser. No. 51, Sijthoff Noordhoff, Gronigen, p. 285 (1981).
Villermaux, J., "Mixing in Chemical Reactors," *ACS Symp. Ser.*, **226**, 135 (1983).
Villermaux, J., "Micromixing Phenomena in Stirred Reactors," *Encyclopedia of Fluid Mechanics*, Gulf Publishing, Houston, p. 707 (1986a).
Villermaux, J., "Macro and Micromixing Phenomena in Chemical Reactors," *Chemical Reactor Design and Technology*, H. I. de Lasa, ed., NATO ASI Series E: Applied Science No. 110, Martinus Nijhoff Publishers, p. 191 (1986b).
Villermaux, J., "Precipitation Reaction Engineering," *Industrial Crystallization*, A. Mersmann, ed., Garmisch-Partenkirchen, Germany, p. 157 (1990).
Villermaux, J., and J. C. Devillon, "Représentation de la Coalescence et de la Redispersion des Domaines de Ségrégation dans un Fluide par un Modèle d'Interaction Phénoménologique," in *Proc. Int. Symp. Chem. Reaction Eng.*, Amsterdam, p. B1-13 (1972).
Zwietering, T. N. "The Degree of Mixing in Continuous Flow Systems," *Chem. Eng. Sci.*, **11**, 1 (1959).

Manuscript received June 30, 1994, and revision received Dec. 13, 1994.